Quantification of biodegradation rate of hydrocarbons in a contaminated aquifer by CO2 δ13C monitoring at ground surface

Christophe Guimbaud, Stéfan Colombano, Cécile Noel, Elicia Verardo, Agnès Grossel, Line Jourdain, Fabrice Jégou, Zhen Hu, Jérémy Jacob, Ioannis Ignatiadis, et al.

Journal of Contaminant Hydrology xxx (xxxx) 104168

Contents lists available at ScienceDirect

Journal of Contaminant Hydrology

journal homepage: www.elsevier.com/locate/jconhyd

Quantification of biodegradation rate of hydrocarbons in a contaminated aquifer by CO_2 $\delta^{13}C$ monitoring at ground surface

Christophe Guimbaud [a, *], Stéfan Colombano [b], Cécile Noel [a, b, 1], Elicia Verardo [c, 2], Agnès Grossel [d], Line Jourdain [a], Fabrice Jégou [a], Zhen Hu [e], Jérémy Jacob [f], Ioannis Ignatiadis [b], Michaela Blessing [b], Jean Christophe Gourry [b]

[a] Laboratoire de Physique et de Chimie de l'Environnement et de l'Espace (LPC2E), CNRS et Université d'Orléans (UMR 7328), 3A av. de la recherche scientifique, 45071 Orléans cedex 2, France
[b] Bureau de Recherches Géologiques et Minières (BRGM), 3 av. Claude Guillemin, 45060 Orléans cedex 2, France
[c] Ecole Nationale Supérieure en Environnement, Géoressources et Ingénierie du Développement durable (ENSEGID), Université Bordeaux III, France
[d] Institut National de la Recherche pour l'Agriculture, l'Alimentation et l'Environnement (INRAE), UR 0272 Science du sol, Centre de recherche d'Orléans, CS 40001 Ardon, 45075 Orléans cedex, France
[e] Shandong Key Laboratory of Water Pollution Control and Resource Reuse, School of Environmental Science and Engineering, Shandong University, Qingdao 266237, China
[f] Laboratoire des Sciences du Climat et de l'Environnement, UMR 8212 CNRS-CEA-UVSQ, Domaine du CNRS, 91198 Gif sur Yvette, France

ARTICLE INFO

Keywords:
Groundwater bioremediation
Hydrocarbon-BTEX
IRIS
$\delta^{13}C_{CO2}$
$\delta^{13}C_{TOLUENE}$
Rayleigh eqs

ABSTRACT

Ground surface analysis of CO_2 emissions with $\delta^{13}C$ determination is experimentally demonstrated to be a potential methodology to monitor, *on line,* the dynamics of petroleum-hydrocarbon biodegradation in soil aquifers, thanks to the improvement of the *Isotopic Ratio Infra Red Spectroscopy* technique. Biodegradation rate of remaining hydrocarbon substrates in groundwater can be quantified using basic application of the *Rayleigh* equations, by $\delta^{13}C_{CO2}$ analysis released at ground surface above the pollution plume instead of usual approaches based on groundwater hydrocarbons $\delta^{13}C$ analysis, when physical and chemical properties for the contaminated site meet appropriate conditions.

The validation approach for that gasoline contaminated specific site is discussed and verified by comparison of first order attenuation rate constant determined from $\delta^{13}C_{CO2}$ analysis emitted at ground surface and from $\delta^{13}C_{TOLUENE}$ analysis in ground water. A kinetic fractionation factor α of 0.9979 (or ε value of −2.1 ± 0.5‰) is estimated for the biodegradation of the most reactive hydrocarbon substrates (TEX). The treatment of this *Rayleigh* equations by linear regression of $\delta^{13}C_{CO2}$ values along the predominant direction of groundwater flow leads to the following results and conclusions for that site: (i) first order biodegradation rate constants (and annual variation) are maximum after the activation of a Permeable Reactive Barrier (PRB) in May 2014: 0.92(+0.29–0.17) $year^{-1}$, and during July and October: 0.46(+0.14–0.09) $year^{-1}$ and minimum in mid-winter in February 2015: 0.17(+0.05–0.03) $year^{-1}$, given by the estimation range for ε. These results are in the lower range with reported in literature for similar contaminated sites (1.6–18 $year^{-1}$) considering natural attenuation under sulfate reducing conditions and (ii) the seasonal variation of the first order biodegradation rate constant is mainly correlated with the seasonal variation of the CO_2 flux, where maximum values are in summers and minimum values in winters. Both seasonal variations are mainly due to the annual cycle of the natural biodegradation activity at the scale of the pollution plume, rather than the activation of the PRB.

This work demonstrates that $\delta^{13}C_{CO2}$ analysis released at ground surface from biodegradation of groundwater hydrocarbons could provide, under characterized and appropriate conditions, a non-intrusive (without soil samplings), fast, and low-cost online method to monitor and therefore to optimize soil remediation processes in real time. (Monitored Natural Attenuation or Enhanced Bioremediation).

* Corresponding author.
E-mail address: christophe.guimbaud@cnrs-orleans.fr (C. Guimbaud).
[1] now at Bureau Veritas Exploitation,333 avenue Georges Clemenceau,
[2] now at WSP France

https://doi.org/10.1016/j.jconhyd.2023.104168
Received 29 August 2022; Received in revised form 25 February 2023; Accepted 27 February 2023
0169-7722/

1. Introduction and challenges

Spills or leaks of petroleum hydrocarbons from gasoline station lead to contamination of soil and groundwater especially by Benzene, Toluene, Ethylbenzene, Xylene (BTEX) compounds. BTEX are the most toxic petroleum hydrocarbons and are usually the primary drivers for remediation (Barona et al., 2007; El-Naas et al., 2014). Monitored Natural Attenuation or Enhanced Bioremediation of BTEX are two major site remediation technologies that rely on the occurrence of biodegradation. Biodegradation processes of hydrocarbons (substrates) by micro-organisms usually induces unidirectional reactions (hydrocarbons to the biologically-mediated product or final product such as CO_2) with isotope fractionation of carbon (C), involving an increase of the isotopic ratio $^{13}C/^{12}C$, R_S, in the remaining substrate (S) and a decrease of the isotopic ratio $^{13}C/^{12}C$, R_P, in the released product (P).

Associated kinetic fractionation factor α is expressed as in Mariotti et al. (1981):

$$\alpha = \alpha_{PS} = R_P/R_S \quad \text{(Eq. 1)}$$

Isotope $\delta^{13}C$ values are more often used than isotope R values for sample data analysis and discussion. $\delta^{13}C$ value is defined for any sample according to Eq. 2:

$$\delta^{13}C\,(‰) = \left(R/R_{VPDB} - 1\right) \times 1000 \quad \text{(Eq. 2)}$$

where, R and R_{VPDB} are the isotopic concentration ratios $^{13}C/^{12}C$ of the groundwater sample and of the international standard, the *Vienna Pee Dee Belemnite*, respectively. R_{VPDB} is 1.12372%, as defined by Craig (1954).

The isotopic fractionation of groundwater hydrocarbon substrate can be described using a simple *Rayleigh* model, which was originally derived by Rayleigh (1896) for the case of fractional distillation of mixed liquid, using the following equation:

$$R_{S,t1}/R_{S,t0} = \left(N_{S,t1}/N_{S,t0}\right)^{(\alpha-1)} = f_{(t1-t0)}{}^{(\alpha-1)} \quad \text{(Eq. 3)}$$

where $R_{S,t1}$ and $R_{S,0}$ are the $^{13}C/^{12}C$ of the unreacted substrate S at time t1 and at the initial time t0, respectively, $N_{S,t1}$ and $N_{S,t0}$ are the molar or molecule number of the unreacted S at time t1 relative to time t0, and thus $f_{(t1\text{-}t0)}$ is the molar or mass fraction of S remaining in the sample at time t1 relative to t0, measured in a well-mixed-aquifer, considering a closed system for the substrate, not movable, or movable such as a plume carried by the stream of ground water. The Rayleigh model is used to quantify the degradation of a single substrate in a well-mixed aquifer to a single product assuming that other non-degradative physical processes such as dissolution, sorption, and volatilization do not cause large carbon isotopic shifts at equilibrium (Mariotti et al., 1981).

U.S. EPA. (2008) guidance document on CSIA discusses how to use and interpret compound specific stable isotope data in field settings using *Rayleigh* model in a groundwater plume. In all discussion provided in Sections 3.3, 4.2, Table 4.2, 5.3 and 7.4. of the U.S. EPA. (2008) document, it is assumed that the difference in isotopic signature between two points A (Source or upgradient monitoring point) and B (downgradient monitoring point) at a snapshot in time (t) in a groundwater plume is due to the transformation that occurred during the travel time (estimated as distance, L, between spots A and B divided by groundwater velocity, v), as written in **Eqs. 4**. In other words, this use of *Rayleigh* model is similar to changes in isotopic signatures over time for a constituent in a closed system (say lab microcosm or a batch reactor).

$$R^B{}_{S,t}/R^A{}_{S,t} = \left(N^B{}_{S,t}/N^A{}_{S,t}\right)^{(\alpha-1)} = f_t^{(\alpha-1)} \quad \text{(Eq. 4)}$$

To estimate the mass loss of S of groundwater hydrocarbon substrates by $\delta^{13}C$ analysis within the plume, the remaining substrate mass fraction (f_t) at time t between two spots A and B can be derived from the kinetic fractionation factor α measured in laboratories (or assessed under field conditions) and the isotopic concentration ratio $^{13}C/^{12}C$ of S, $R^A{}_S$ or $R^B{}_S$, measured in observation wells A and B at time t, with suffix t removed from latter equations.

$$f = \left[R^B{}_S/R^A{}_S\right]^{1/(\alpha-1)}$$
$$f = \left[\left(\delta^{13}C^B{}_S + 1000\right) / \left(\delta^{13}C^A{}_S + 1000\right)\right]^{1000/\varepsilon} \quad \text{(Eq. 5)}$$

with $\varepsilon = (\alpha - 1).1000$, being the associated isotope fractionation factor expressed in ‰,

Eqs. 5 are identical to Eq. 7.17 in the U.S. EPA. (2008) guidance document on CSIA. The extent of the hydrocarbon biodegradation could be expressed as the % Mass Loss of S in the time interval t, (ML_t), as expressed in Eq. 6, to discuss in later section one of the boundary condition limiting the use of this Rayleigh equation form.

$$ML\ [\%] = (1\text{–}f) \times 100 \quad \text{(Eq. 6)}$$

The evolution of ML over time is also a key parameter to estimate the time to achieve groundwater objectives due to natural or enhanced bioremediation of hydrocarbons contaminated aquifers.

The main inconvenient of this monitoring approach based on hydrocarbon substrate pollutants concentration and δ determination is that monitoring wells to be drilled for sampling groundwater are needed.

It has been suggested that monitoring the isotope $\delta^{13}C$ values of the biodegradation product P═CO_2 (labeled $\delta^{13}C_{CO2}$ or $\delta^{13}C_P$) released at ground surface, as a proxy of the hydrocarbon substrate pollutant δ values, could be a more convenient way to assess the groundwater hydrocarbon biodegradation kinetic within high spatial and temporal resolutions. Within the latter approach, soil drilling or excavation is not needed. The *Keeling* plot method to measure δ values of the biodegradation product P═CO_2 released at ground surface only requires a movable closed chamber set on ground surface where δ values of the accumulated CO_2 gas is directly measured online by Isotopic Ratio Infra Red Spectroscopy (IRIS) technique (Noel et al., 2016a, 2016b; Guimbaud et al., 2016), only for few minutes thanks to the precision improvements made by IRIS techniques in the last decades in the gas phase.

This paper aims to demonstrate that the biodegradation efficiency of hydrocarbons in a gasoline contaminated aquifer (under Monitored Natural Attenuation or Enhanced Bioremediation) could be monitored by ground surface δ_{CO2} emissions. As a first approximation, improving then the ability to observe and assess quickly effects of remediation processes that could be applied in the field. Boundary conditions for the application of the *Rayleigh* model to assess biodegradation rate of the groundwater hydrocarbon substrates from ground surface $\delta^{13}C_{CO2}$ emissions is discussed at the scale of the contaminated field.

2. Material and methods and theory/calculation

2.1. Characterization of the investigating site

The site widely described in Verardo (2016) and Verardo et al. (2021) is a gas station near Paris (France) where gasoline and diesel fuels leaked from tanks. A simplified map of the site showing the Permeable Reactive Barrier (PRB) and the monitoring disposal of the gas metering station is presented in Fig. 1. A Permeable Reactive Barrier (PRB) was implemented 22 m downstream of the pollution source to stimulate biodegradation, started on march 27, 2014 and ended on June 26, 2015. Diluted H_2O_2 is added continuously to pumped water from wells located upstream the PRB. Then, oxygenated pumped water was injected across the PRB.

That industrial site is composed of sandy and gravelly materials (1.5 m thick at surface) and of a sandy lightly loamy layer containing mainly gritstone (coarse-grained of siliceous sandstone from Brie-

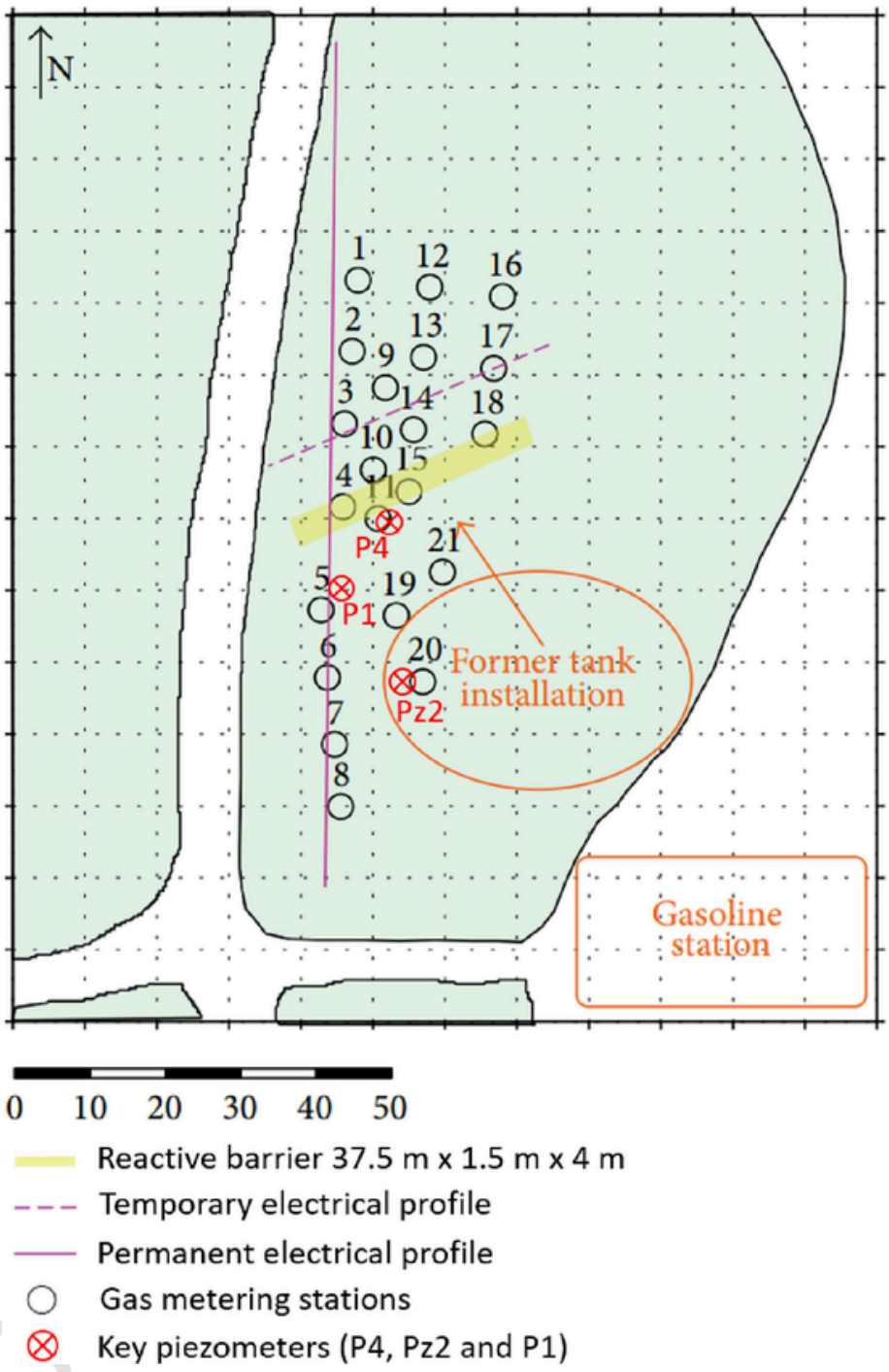

Fig. 1. Map of the site showing the reactive barrier and the monitoring disposal. Each number (1–21) refers to a collar number for gas metering stations (extracted form Noel et al., 2016b).

Region) above 6 m depth. The aquifer layer varies from 2 to 3 m depth on top (from end of winter to end of summer) and lies above the impermeable soil layer at 6 m depth. The gas station is still in activity but the former tank (source of contamination) was removed in 1997. Since that time, a large reservoir of residual hydrocarbons located in the vadose zone (just below the former tanks) is continuously feeding the underneath groundwater with refined petroleum. Residual Light non-aqueous phase liquid (LNAPL) was found in soil between 2 and 4 m depth at saturation range between 0.5 and 2.4%. Localization of the residual LNAPL is shown in Fig. 2, where collars 19, 20 and 21 are the only ones located above the residual LNAPL area, ending upstream collar 11. From these observations, the simplifying assumption that groundwater system is 'well mixed' will be considered upstream and downstream the PRB to estimate the mass loss of hydrocarbon substrates and their attenuation rate constant. Actually, the pollution plume in groundwater is mainly composed of BTEX due to their longer resistance to biodegradation and their higher solubility, compared to other hydrocarbons (Verardo et al., 2021). Groundwater analysis performed from 2012 to 2014 at the exit of the pollution plume (monitoring well P4, Fig. 2, located 5 m upstream the front head of the PRB, 4 m upstream collar 11 and 17 m downstream the dismantled tanks in 1997) indicates max values of pollutants from the layer depth 2 m–4 m below soil surface, with

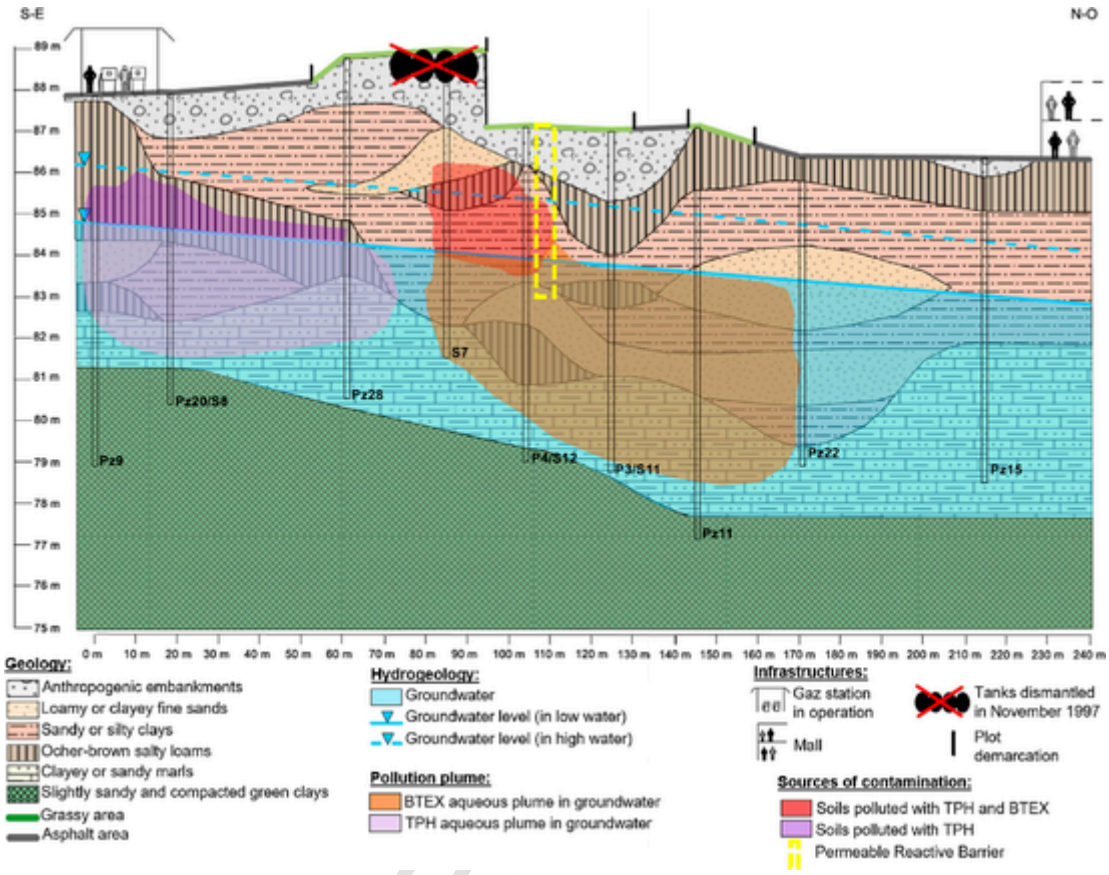

Fig. 2. Hydrogeological conceptual model of the site.

max values (Verardo et al., 2021) for Benzene (11 mgL^{-1}), Toluene (3 mgL^{-1}), Ethylbenzene (1 mgL^{-1}), and Xylene (6 mgL^{-1}). Total Petroleum Hydrocarbon (TPH) C10-C40 and MTBE (Methyl tert-butyl ether) concentration max values are 1 mgL^{-1} and 100 μgL^{-1}, respectively. BTEX distribution, extracted from Verardo, 2016, is shown in Fig. 3. BTEX are sampled from static headspace and analyzed by GC–MS according to the NF ISO 11423-1 protocol with quantification limit of 1 μgL^{-1}. TPH are sampled from liquid-liquid extraction and analyzed by CG-FID according to the NF EN ISO 9377-2 protocol. Accuracy varied from 30 to 50% (Blessing and Saada, 2013).

The biodegradation of BTEX can be carried out under aerobic, anoxic or anaerobic conditions. In aerobic respiration, the terminal electron acceptors (TEA) is O_2, but in the absence of oxygen, a number of less highly oxidized compounds may serve, assuming organisms capable of making use of them are present. Available TEAs are used in the environment in decreasing order of oxidation–reduction potential (NO_3^-, Fe(III), Mn(IV), SO_4^{2-}, and CO_2) (Davis et al., 1999; Johnson et al., 2003; Lari et al., 2019). Groundwater at the contaminant plume is anaerobic, as shown in Fig. 4 extracted from Verardo (2016). The concentrations of nitrates, iron II, manganese II and sulphates measured in the groundwater of the site made it possible to define the redox zones of biodegradation of hydrocarbons. The biodegradation mechanisms existing within the plume of contaminants are also presented in Fig. 4, demonstrating that hydrocarbon biodegradation remains processed via anaerobic conditions and more precisely via sulfate reduction before enhanced bioremediation along the pollution plume, mainly within the gas metering station zone . After activation of the PRB, no evolution of the redox potential (stable between −100 and − 50 mV) in the piezometers located near PRB was noticed, despite the injection of hydrogen peroxide. This result and the presence of sulphates, absence of manganese II production and low Iron II production demonstrate that biodegradation remains anaerobic and processed via sulfate reduction due to a default of treatment (Verardo, 2016). According to these lower limits of redox potential, biodegradation seems not to proceed via methanogenenis. This could be notified by the absence of methane realized at ground surface (< 0.1 nmol m^{-2} s^{-1}) at one most active period (July 1, 2015), corresponding the detection limit of the IR Greenhouse Gas Analyzer (Los Gatos Research, Inc. CA) used and at least to one order of magnitude lower than fluxes which can be found in literature for water bodies or aerobic soil surfaces (Guimbaud et al., 2016). However, hydrocarbon biodegradation under acetoclastic and hydrogenotrophic reducing conditions (methanogenesis) may not be ignored within the residual LNAPL (light non-aqueous phase liquid) source zone located upstream the PRB according to high BTEX concentration found in Fig. 4 (Conrad et al., 1997). These methanogenesis paths are known to produce high $\delta^{13}C$ values (^{13}C enrichment) of both CO_2 and CH_4 gas and DIC and dissolved methane in groundwater. In addition, aerobic oxidation of overlying CH_4 in the vadose zone may also produce additional ^{13}C enrichment of CO_2 (Conrad et al., 1997; Neumann et al., 2016, and references therein). Despite concentration change in redox indicator compounds do not play for significant methanogenesis processes, the $\delta^{13}C$ value decays less upstream than downstream the PRB (~ -2.5‰ versus ~ -4‰VPDB, Guimbaud et al., 2016). It implies that higher $\delta^{13}C$-CO_2 could be produced upstream the PRB from methanogenesis, reducing then this $\delta^{13}C$ value decays observed. The kinetic approach given in that paper is thus limited by the relative importance of CO_2 produced methanogenesis paths in residual LNAPL zone. Methanogenesis is assumed to be neglected in our study case, as data including the LNAPL zone do not affect the general trend of $\delta^{13}C$-CO_2 and BTEX. In order to assess the significance of CO_2 contribution by (in)direct methanogenesis, Conrad et al., 1997, suggested that combined $\delta^{13}C$ and ^{14}C analyses of soil CO_2 gas and groundwater DIC can yield to valuable insights into modes of microbial petroleum hydrocarbon degradation.

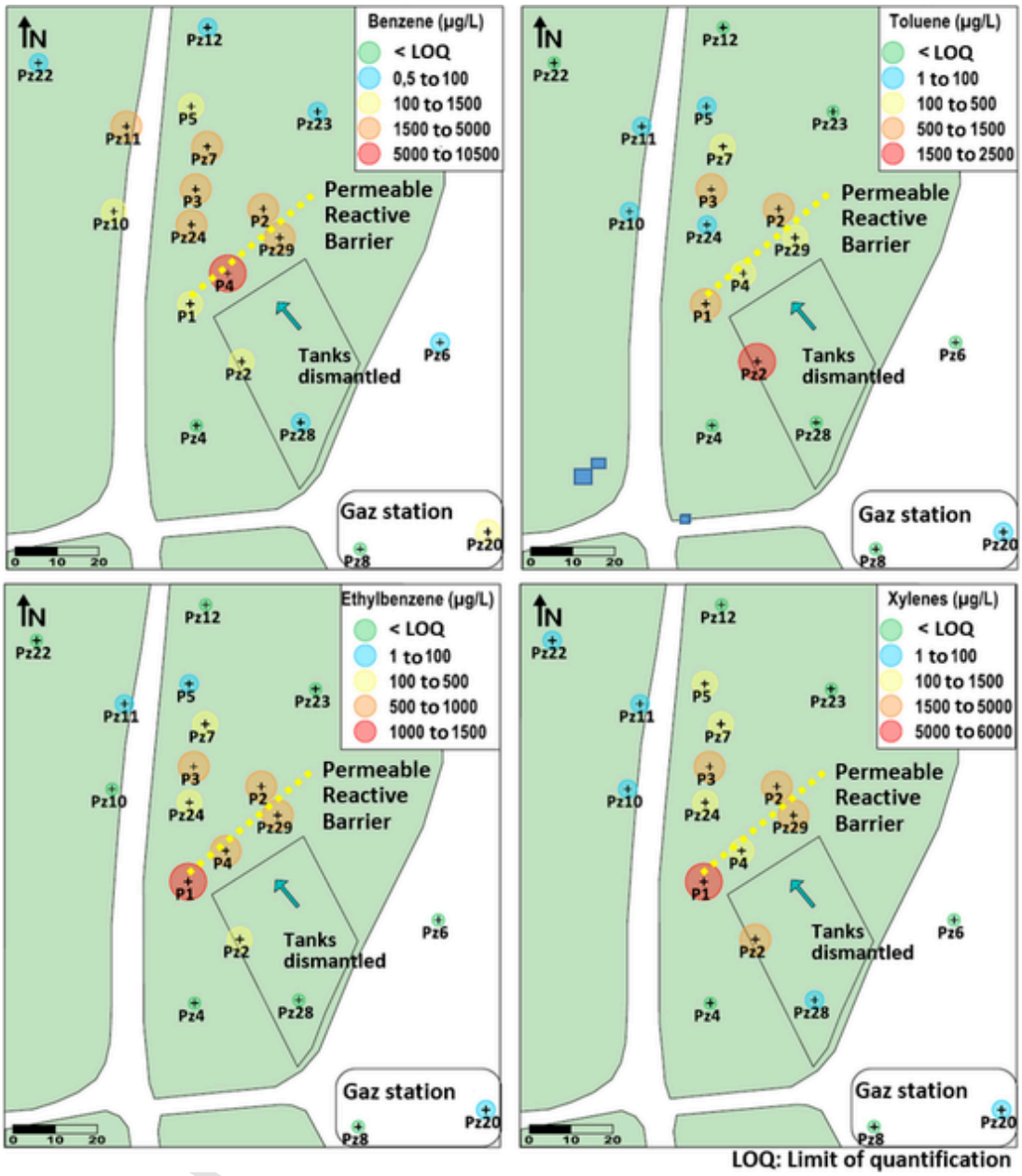

Fig. 3. Representative or average concentrations of benzene, toluene, ethylbenzene and xylenes in the groundwater of the site before the treatment phase between June 2012 and February 2014 (the limits of quantification (LOQ) are 0.5 µg/L for benzene and 1 µg/L for TEX).

Geophysical methods (electrical resistivity and induced polarization) had shown a high conductive and chargeable zone, around 2 to 3 m depth, which matches the polluted zone defined by geochemical borehole analyses, at the top layer of the water table (Noel et al., 2016b). Authors conclude that pollutant degradation mainly occurs in the top layer of the groundwater table where numerous chargeable bacteria produce conductive metabolites. The age of the hydrocarbon leakage (almost twenty years ago) is sufficient to allow the development of natural bacterial flora able to degrade hydrocarbon.

The direction of the groundwater flow is oriented toward the northwest by 30° relative to the north (Fig. 1) and obtained from piezometric maps using *krigeage* interpolation. This direction defines also the pollution plume coordinate relative to the PRB (Verardo, 2016). The average groundwater velocity (17 m yr^{-1}) is derived from the kinematic porosity of 15%, the hydraulic gradient of 1% and an average hydraulic conductivity of 8.10^{-6} m s^{-1} measured in that site.

Material and methods for CO_2 flux and $\delta^{13}C$ characterization on each 21 gaz metric station (see Fig.1 for the position of the 21 collars set on ground surface) are described in Guimbaud et al. (2016). LPC2E-CNRS developed home built high-resolution infra-red spectrometers, which performances are discussed elsewhere (Guimbaud et al., 2011, Guimbaud et al., 2016; Catoire et al., 2017), among them the IRIS instrument named SPIRIT-BIOPHY to measure CO_2 volume mixing ratio and $\delta^{13}C$ released at ground surface (Guimbaud et al., 2016). Measurements were made using the closed chamber method and the *Keeling* plot approach (Pataki et al., 2003). Precision and accuracy for $\delta^{13}C_{CO2}$ usually varies from 0.15‰ to 0.5 ‰ from a single *Keeling* plot extraction, with best precision obtained for high CO_2 flux intensity (in summer) and for high temperature stability of the instrument (under cloudy and low wind periods).

It has been shown (Guimbaud et al., 2016; Noel et al., 2016b) that, before and after biodegradation stimulation, a correlation is observed (from upstream to downstream the pollution plume) between (i) CO_2

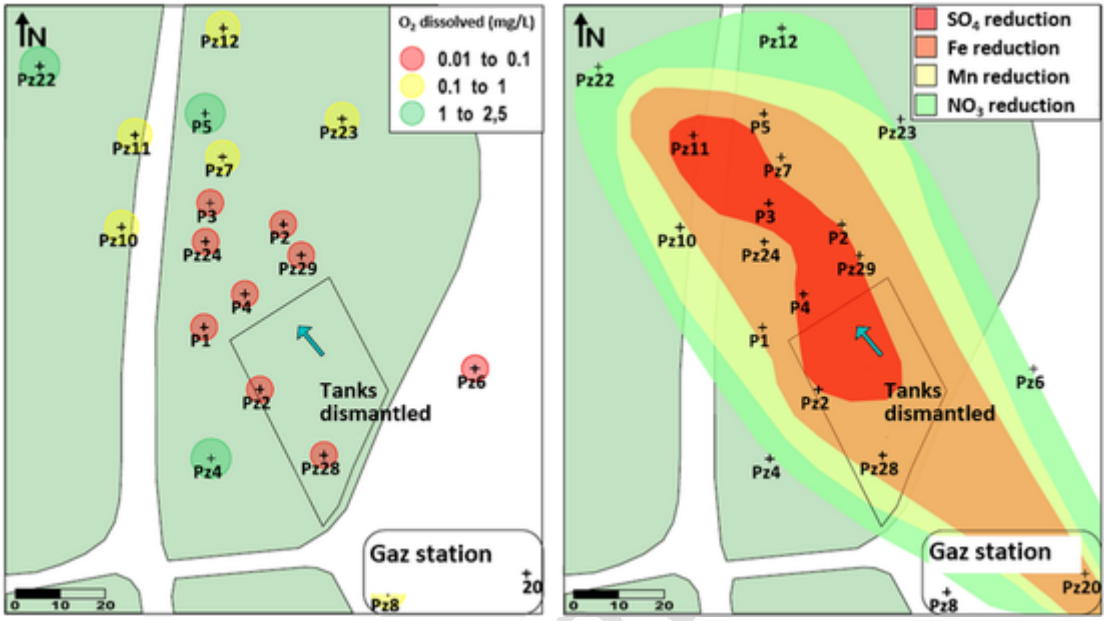

Fig. 4. Left: average dissolved O_2 concentrations at a depth of 3 m below the static level, recorded in September 2013 and February 2014; On the right: redox zone of biodegradation of petroleum hydrocarbons established from the concentrations of sulphates, iron II, manganese II and nitrates measured in the groundwater between June 2012 and February 2014.

flux emitted at the surface and the BTEX concentration in the aquifer and (ii) $\delta^{13}C$ values of CO_2 emitted at the surface ($\delta^{13}C_{CO2}$) and $\delta^{13}C$ values of BTEX in groundwater ($\delta^{13}C_{BTEX}$), as representative main hydrocarbons in that site. From upstream to downstream the pollution plume, $\delta^{13}C_{CO2}$ values at ground surface are correlated with $\delta^{13}C$ values of BTEX hydrocarbons (Benzene B, and Toluene T in that site) in the aquifer, with a difference Δ ($\delta^{13}C_{CO2} - \delta^{13}C_{BT}$) ≈ -3 ‰, mainly for toluene (See Guimbaud et al., 2016 and result section). This difference observed is mainly due to preferential selection of light isotopes (^{12}C) during bacterial metabolism, hydrocarbon redox degradation pathways, and hence release of ^{13}C-depleted CO_2, slightly magnified by fractionation during vertical diffusion of CO_2 to the surface, assuming that no other fractionation process occurs. Other fractionation processes leading to high $\delta^{13}C$-CO_2 may interact and complexify the system (Conrad et al., 1997), such as CO_2 issued from atmospheric contamination, CO_2 produced from methanogenic activity, dissolution of carbonate minerals, biodegradation of endogenous soil organic matter).

Such depleted $\delta^{13}C_{CO2}$ values observed in that site could indicate that hydrocarbon biodegradation occurs via sulfate reduction (Conrad et al., 1997; Landmeyer et al., 1996; Wanner et al., 2019). The Guide for assessing biodegradation and source identification of organic ground water contaminants using Compound Specific Isotope Analysis (CSIA) from the United States Environmental Protection Agency (U.S. EPA., 2008) provides the recommended isotope enrichment factors (ε_{PS}) under sulfate reducing conditions for main BTEX ranging from −3.7‰ to −0.8‰, as summarized in Table 1.

It is commonly observed that the rate of benzene biodegradation is much slower than TEX and other petroleum hydrocarbon constituents under anaerobic conditions (Atteia and Guillot, 2007; Guimbaud et al., 2016; Kolhatkar and Schnobrich, 2017; Toth et al., 2021; Sra et al., 2022). Half-lives for natural degradation of gasoline compounds in anaerobic groundwater under sulfate reducing conditions were found to be larger than 800 days for benzene, significantly higher than for other TEX: 230 days for ethylbenzene, 120 days for Toluene, 125 to 180 days for Xylenes, and 160 to 180 days for Naphthalene and Trimethylbenzene (Thierrin et al., 1993), equivalent to first order attenuation rates <0.5 year^{-1} for benzene and 1.6 to 3.0 year^{-1} for TEX. Kolhatkar and Schnobrich (2017) reported natural attenuation rate constants for benzene under sulphate reducing condition

Table 1
Isotope enrichment factor (ε_{PS}) under sulfate reducing conditions for main BTEX Using Compound Specific Isotope Analysis (CSIA) according to U.S. EPA. (2008).

Organic compound	$^{13}C/^{12}C$ fractionation factor ε_{PS} (‰)	References	Bacteria
Benzene	−3.6	Mancini et al., 2003	Enrichment culture
Toluene	−0.8	Ahad et al., 2000	Enrichment culture
Toluene	−1.5	Meckenstock et al., 1999	Column experiment
Toluene	−2.2	Morasch et al., 2001	*Desulfobacterium cetonicum*
Toluene	−1.7	Meckenstock et al., 1999	Strain TRM1
Ethylbenzene	−3.7	Wilkes et al., 2000	Enrichment culture
m-Xylene	−1.8	Morasch et al., 2004	Strain OX39
o-Xylene	−1.1	Richnow et al., 2003	Column experiment
o-Xylene	−3.2	Wilkes et al., 2000	Enrichment culture

ε_{PS} is the Isotope enrichment factor for the entire molecule of substrate S with: $\varepsilon_{PS} = (\alpha_{PS} - 1)0.1000 = (K_H/K_L - 1)0.1000$; α_{PS} is the isotope fractionation enrichment factor given by the ratio of the rate constant for reaction of molecules with a heavy isotope (K_H) anywhere in the molecule (substrate S) compared to the rate constant for reaction of molecules with light isotopes only (K_L)).

0.20–0.46 year^{-1}. Under such conditions, Verardo (2016) reported from literature review first order natural degradation rates 1 to 2 order of magnitude lower for benzene, 1.8 × 10^{-2}–1.8 year^{-1}, than for TEX, 1.8–18 year^{-1}).

Due to the higher concentration of TEX in the pollution plume and to the higher reactivity of TEX (having similar first order attenuation rates) than benzene, it is considered that attenuation is mainly due from these most abundant and reactive species, where TEX have also similar $\delta^{13}C_{hydrocarbon}$ value (see next section) and similar estimated attenuation first order rate constants under sulfate reducing conditions. An ε_{PS} range is found to be −2.1‰ with a mean deviation of ± − 0.5‰ for typical concentration values 9/3/1 for X/T/E respectively using ε_{PS} from Table 1 given from the CSIA data base (U.S. EPA., 2008).

2.2. Approach to monitor the biodegradation rate of hydrocarbon substrates by $\delta^{13}C_{CO2}$ analysis released from ground surface within an expanding plume

The quantification of pollutant substrate biodegradation efficiency within an expanding plume from the source to an observation well using solution of *Rayleigh* model based on single substrate concentration and δ analysis is well documented (Richnow et al., 2003; Fischer et al., 2007; Thullner et al., 2012; Denk et al., 2017; Van Breukelen, 2007a; Van Breukelen, 2007b). Boundary conditions for the application of the *Rayleigh* model are given from assumption (A) 1 to 3:

(A1) The pollutant plume is only fed by the dissolution of the hydrocarbon source located upstream in the former gasoline tank area and groundwater pollutants are well-mixed systems downstream the area of extension the LNAPL, as discussed in Verardo (2016).

(A2) Biodegradation is the dominant process over others affecting the dissolved pollutant migration such as volatilization or sorption-desorption, as discussed in Verardo (2016).

(A3) Low percentage mass loss of substrate should occurs from two monitoring wells or during migration of the plume within the period of investigation, ideally considered below 10% to assume mass balance conservation made a boundary condition for this derived form of the *Rayleigh* equation.

Additional Boundary conditions or hypothesis are required to assess biodegradation rate of the groundwater hydrocarbon substrates from ground surface δ_{CO2} emissions analysis.

In real conditions, hydrocarbon pollutants in contaminated aquifer are present as a mixture. Biodegradation kinetic fractionation factor α depends mainly on the chemical composition of hydrocarbon contaminant and biochemical pathways of biodegradation associated with redox conditions. To assess an average dynamic for a pool of hydrocarbons substrate biodegradation in contaminated aquifer, one can assume (A4) that considered contaminants starts with similar average initial δ value, same biodegradation rate, and same α_{PS} (P═CO_2 resulting from biodegradation of S substrates).

This site is characterized by close δ values of BTEX: benzene (−28‰), toluene and m-p Xylenes (−27.5‰) and ethyl benzene (−27‰) upstream/nearby the PRB, with isotopic enrichment from 0.5 to 1 ‰ after bioactivation of the PBR, the highest for toluene (Verardo, 2016). A common biodegradation rate could be assumed in previous section for the largest pool of reactive substrates with a common kinetic fractionation factor $\alpha = 0.9979$ or $\varepsilon = -2.1‰$.

The apparent fractionation factor α_{app} from the transformation of the hydrocarbon substrate S solubilized in the top layer of groundwater to CO_2 product P released to the atmosphere ground surface is given by:

$$\alpha_{app} = {R^X}_P / {R^X}_S \quad \text{(Eq. 7)}$$

where the substrate S concentration in groundwater at spot X along the main migration axis at time t is given by $C^X_{S,t}$ and the isotopic concentration ratio $^{13}C/^{12}C$ of S in groundwater and of the biodegradation product (P = CO_2) released at soil surface to the atmosphere are given by ${R^X}_S$ and ${R^X}_P$, respectively.

α_{app} results from the kinetic fractionation factor of P relative to S in the water aquifer, α, and from the fractionation factor due to selective vertical diffusion of the lighter isotope of CO_2 product from the top layer of groundwater to the ground surface, α_{diff}, if one assume (A5) that the source of CO_2 released at ground surface from hydrocarbons biodegradation at water table of the aquifer should be dominant versus CO_2 released from other potential sources such as CO_2 issued from atmospheric contamination, (i) dissolution/precipitation of carbonate minerals, (ii) biodegradation of endogenous soil organic matter, reducing then the effect of other type of fractionation processes.

(i) The groundwater is also in equilibrium with calcite (Verardo, 2016), meaning that there is no precipitation of carbonate or dissolution of from sediment which could affect the content of mineral carbon in the aquifers and its isotopic composition. The aquifer is characterized by high alkalinity (5×10^{-3} M) with a stable pH (6.8), with no significant changes after biostimulation. During treatment, **anaerobic** conditions remained mainly unchanged as regards O_2 dissolved concentration collected from P1, P2 and Pz29 relative to data shown in Fig. 4 (left panel) just before treatment (February 2014), except for P4 above the PRB at the beginning and at the end of treatment, where O_2 dissolved concentration could reach 5 mg L^{-1} (Verardo, 2016). (ii) Possible competition and seasonal effects occurring for the natural soil respiration and petroleum hydrocarbon biodegradation (BenIsrael et al., 2019; Wanner et al., 2019). In this specific site, natural soil respiration can be neglected due to the low amount of organic matter inside the soil. Surface vegetation is homogeneous, covered by a layer of grass during the high vegetation season which almost disappears during the winter season. In order to minimize the contribution of natural soil respiration the 15 cm top layer of the ground surface was removed before installation of collars into the soil for each metering station. CO_2 fluxes from uncontaminated or less contaminated area (collars 7 and 8 located out of the contamination plume) vary from ~0.7 to 2.5 μmol m^{-2} s^{-1}) from end of winter to summer. This is assumed to be the maximum contribution of soil respiration or other processes of CO_2 released above the hydrocarbon underground layer. As a consequence, fluxes observed under contaminated areas with typical values varying from 5 to 45 μmol m^{-2}·s^{-1} imply that CO_2 natural soil respiration represents at most 5% of CO_2 emissions relative to hydrocarbon biodegradation, from winter to summer. As a consequence, under that specific site, the low emissions levels of CO_2 outside the pollution plume imply that the fraction of CO_2 emissions issued from natural soil respiration is assumed to be negligible compared to CO_2 emitted from gasoline hydrocarbon biodegradation.

Previous studies revealed that diffusion through the non-saturated zone could lead to isotope distillation effects with negative Δ values for CO_2 (Cerling et al., 1991) and for organic compounds (Bouchard et al., 2008a; Bouchard et al., 2008b); the isotope effect due to CO_2 volatilization in the non-saturated zone to soil surface is assessed by measuring gas phase $\delta^{13}C_{CO2}$ directly on top of the water table (through monitoring wells above the reactive barriers to bypass the underground soil intermediate) and $\delta^{13}C_{CO2}$ on soil surface (i.e., from closest collars). July 2014 data provides $\delta^{13}C_{CO2}$ values of (−29.2‰ ± 0.6‰ VPDB) from monitoring wells versus (−29.9 ± 0.4‰ VPDB) from collars surrounding the reactive barriers, respectively. Values are found to be more spread (−28.4‰ ± 0.7‰ VPDB) versus (−29.2 ± 0.5‰ VPDB) in October 2014. This indicate vertical diffusion Δ_{diff} value of ~ −0.7‰ leading to a vertical diffusion fractionation factor α_{diff} value of ~0.9993. Therefore, possible negative Δ values fractionated CO_2 produced from volatilized fractionated organic compounds in the non-saturated zone is neglected because the loss of organic compounds by volatilization is insignificant relative to their mass balance in the aquifer.

Under our study site α_{app} = 0.997 (obtained from Δ ($\delta^{13}C_{CO2}$ − $\delta^{13}C_{BTEX}$) = −3 ‰) results approximatively from the kinetic fractionation factor of CO_2 relative to TEX estimated in the water aquifer ($\alpha = 0.9979$ or $\varepsilon = -2.1‰$) and from the fractionation factor due to selective vertical diffusion of the lighter isotope of CO_2 product from the top layer of groundwater to the ground surface (α_{diff}, of 0.9993 or $\varepsilon = -0.7‰$), where α_{app} is then given by:

$$\alpha_{app} = \alpha.\alpha_{diff} \quad \text{(Eq. 8)}$$

Among α values, α_{app} is the only assessable variable from field measurable data: δ_P of CO_2 released in atmosphere at ground surface and δ_S of hydrocarbon substrate solubilized in top layer of aquifer. α_{app} can be expressed from Eq. 7:

$$\alpha_{app} = \left(\delta^{13}C_P + 1000\right) / \left(\delta^{13}C_S + 1000\right) \quad \text{(Eq. 9)}$$

α, α_{diff} and thus α_{app} are generally assumed to be invariable with time, t, (Mariotti et al., 1981) and remained constant along the horizontal migration of S at the scale of the pollution plume (A6).

Solving R^B_S and R^A_S from Eq. 7 and replacing into the left member of Eq. 5, yields to Eq. 10, by removal of α_{app}:

$$f = \left(R^B{}_P / R^A{}_P\right)^{1/(\alpha-1)} \quad \text{(Eq. 10a)}$$

$$f = \left[\left(\delta^{13}C^B{}_P + 1000\right) / \left(\delta^{13}C^A{}_P + 1000\right)\right]^{1000/\varepsilon} \quad \text{(Eq. 10b)}$$

with P=CO_2 and

$$\varepsilon = (\alpha - 1).1000 \quad \text{(Eq. 11)}$$

being the associated isotope fractionation factor expressed in ‰.

To support derivation of Eq. 10 from Eqs. 5 and 7, CO_2 realized at ground surface should be directly issued from the biodegradation of the underneath hydrocarbons substrate in the saturated zone, meaning additional assumption are made:

(A7) horizontal migration velocity of the well mixed hydrocarbon substrates is assimilated to the velocity of the groundwater flow, because sorption and desorption are neglected processes in this site.

(A8) Sorption and desorption during advective horizontal and vertical migrations in the saturated zone are not leading to isotope fractionation, as neglected in this site and from discussion in Elsner et al. (2005) and Schmidt et al. (2004).

(A9) vertical diffusion of CO_2 within the unsaturated zone (from top layer of the aquifer to ground surface) is assumed to be "extremely fast" relative to advective (horizontal) migration of CO_2 in the saturated zone (in the aquifer along the pollution plume), according to Abreu and Johnson (2006) and to Luo et al. (2009). Under this site, the soil effective porosity of 15% is known to be characterized by efficient gas transport in air filled pores according to De Robert (2006) where the author also mentioned that CO_2 exchange through water-filled pores is very slow relatively to air filled pores because CO_2 diffusion coefficient in water is 10,000 less than in air.

The percentage of mass loss for a pool of substrates between spot A and B, ML [%], with similar initial δ value and biodegradation rate can be derived from Eq. 12 (assuming A6) if an average α value can be obtained either (i) from field data (by derivation of an α_{app} value from Eq. 7 with measurements $R^X{}_P$, and $R^X{}_S$ followed by assessment of α from Eq. 8, i.e. $\alpha = \alpha_{app}/\alpha_{diff}$) or (ii) from estimated value of α from the CSIA data base (U.S. EPA., 2008). Derivation of ML [%]. From conditions (i) an assessment of α_{diff} is needed from field data to verify assumption A10: $|\alpha_{diff} - 1| << |\alpha - 1|$ or $|\varepsilon_{diff}/1000| << |\varepsilon/1000$, leading then to $\alpha = \sim \alpha_{app}$, where α_{app} is extracted from field study.

The percentage of mass loss from biodegradation for a pool of substrates between spot A and B, ML [%]), is obtained from solving f from Eq. 10, and replacing it into Eq. 6:

$$ML\ [\%] = \left(1 - \left(R^B{}_P / R^A{}_P\right)^{1/(\alpha-1)}\right) \times 100 \quad \text{(Eq. 12a)}$$

$$ML\ [\%] = \left(1 - \left[\left(\delta^{13}C^B{}_P + 1000\right) / \left(\delta^{13}C^A{}_P + 1000\right)\right]^{1000/\varepsilon}\right) \times 100 \quad \text{(Eq. 12b)}$$

As a summary, percentage of mass loss ML [%] from biodegradation of hydrocarbons along a pollution plume, migrating horizontally with the flow of groundwater from spot A to spot B, could be obtained by measuring the isotopic concentration ratio $^{13}C/^{12}C$, R_p, values of the CO_2 product P released at ground surface above spots A and B, at time t, when physical and chemical properties for the contaminated site meet appropriate conditions in addition to the usual approaches based on groundwater hydrocarbons $\delta^{13}C$ substrate S analysis (Eq. 12c),

$$ML\ [\%] = \left(1 - \left[\left(\delta^{13}C^B{}_S + 1000\right) / \left(\delta^{13}C^A{}_S + 1000\right)\right]^{1000/\varepsilon}\right) \times 100 \quad \text{(Eq. 12c)}$$

The first-order kinetic approach of the Monod model is commonly used for remediation site (Bekins et al., 1998; Bauer et al., 2006), with good approximation for upper limits of BTEX concentration of 5 $mg.L^{-1}$, according to Bekins et al. (1998) and Cozzarelli et al. (2010). First-order kinetic approach is used along the pollution plume according to the BTEX mixing ratios monitored in well P4, located 5 m upstream the front head of the PRB (Section II.1).

The estimated first order attenuation rate constant is commonly presented to discuss and compare biodegradation rate in aquifers between 2 monitoring points along a flow path (U.S. EPA., 2008). The first order kinetic assumption is usually an appropriate simplification to describe the biodegradation in aquifers because (i) mass transfer limiting factors are often rate limits in porous media and (ii) Fickian diffusion is a first order process with respect to the substrate concentration in the bulk liquid ((Alvarez De Pedro and Ilman, 2005); Wiedemeier et al., 2007). Biodegradation rate between spot A and spot B is calculated from travelling time t of substrates between the two spots, given by the ratio of the distance L between spots A and B and the horizontal velocity, v, of the substrate migration. Thus, the 1st order biodegradation rate constant, k, is given in Eq. 13e based on the $\delta^{13}C_{CO2}$ product monitoring .

$$N^B{}_S = N^A{}_S.e^{[-k\ t]} \quad \text{(Eq. 13a)}$$

$$\Leftrightarrow k = -\ln\left(N^B{}_S / N^A{}_S\right)/t = -\ln\left(f\right)/t \quad \text{(Eq. 13b)}$$

$$\Leftrightarrow k = -\ln\left[\left(R^B{}_P / R^A{}_P\right)^{1/(\alpha-1)}\right]/t \quad \text{(Eq. 13c)}$$

$$\Leftrightarrow k = +\ln\left(R^A{}_P / R^B{}_P\right) / [(\alpha - 1).t] \quad \text{(Eq. 13d)}$$

$$\Leftrightarrow k = +\ln\left[\left(\delta^{13}C^A{}_P + 1000\right) / \left(\delta^{13}C^B{}_P + 1000\right)\right] / \left[\varepsilon.t/1000\right] \quad \text{(Eq. 13e)}$$

in addition to usual Eq. 13f, based on the $\delta^{13}C_{BTEX}$ substrate monitoring .

$$k = +\ln\left[\left(\delta^{13}C^A{}_s + 1000\right) / \left(\delta^{13}C^B{}_s + 1000\right)\right] / \left[\varepsilon.t/1000\right] \quad \text{(Eq. 13f)}$$

3. Results and discussion: Assessment of the biodegradation rate, BR f(t), of the groundwater hydrocarbon substrates using $\delta^{13}C_{CO2}$ surface analysis

3.1. $\delta^{13}C_{CO2}$ values at the scale of the pollution plume and spatial resolution

This work uses additional data set compared to Guimbaud et al. (2016) from the less bioactive season and new data from the year 2015 period. $\delta^{13}C_{CO2}$ values increase (^{13}C enrichment) as a function of the pollution plume coordinate (Figs. 5 and 6a–c). Fig. 5 shows that $\delta^{13}C$ values of toluene increase by 3.7‰ and 2.1‰ in May and December 2014, respectively, over a distance of 40 m along the pollution plume. In the same conditions, $\delta^{13}C$ values of benzene increase by 1.8‰ and 1.2‰ according also to linear regression given in Fig. 5. This is the consequence of selective biodegradation of the lighter carbon isotope ^{12}C for toluene and benzene leading then to ^{13}C enrichment of toluene and benzene during their migration in the groundwater. The higher ^{13}C enrichment for toluene is due to its faster biodegradation rate than benzene. As a consequence, $\delta^{13}C$ values of CO_2 released at ground surface follows the same trend with and increase by 4.4‰ and 2.7‰ in May and December 2014, respectively. From upstream to downstream the pollution plume, $\delta^{13}C_{CO2}$ values at ground surface are correlated with $\delta^{13}C$ values in groundwater, with a difference Δ ($\delta^{13}C_{CO2}$ -

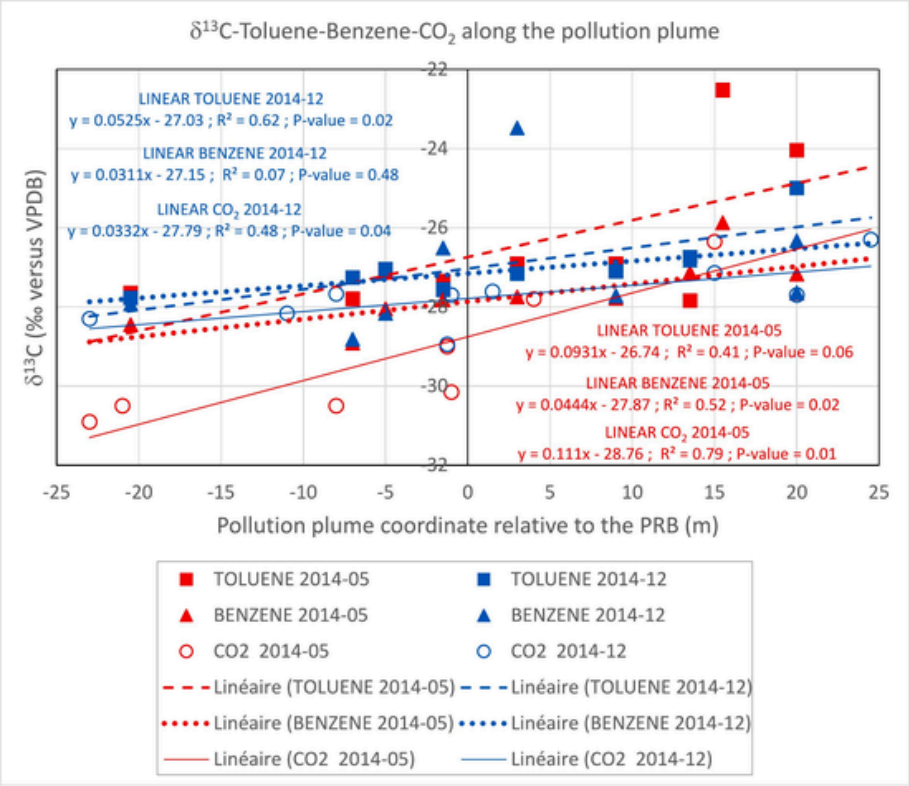

Fig. 5. Ground water $\delta^{13}C$ Toluene-Benzene values sampled from piezometers and surface emitted $\delta^{13}C_{CO2}$ values (‰ versus VPDB as a function of pollution plume coordinate, m), when both data are collected during the same campaign (labeled at the first day of 2 days campaign duration mainly): May and December 2014 campaigns after activation of the Permeable Reactive Barrier (PRB).
The Y axis represents $\delta^{13}C$ values measured for CO_2 emitted at ground surface with a movable flux chamber set on collars (for a 5 to 20 min of duration) of the gas metering station (see Fig.1) or $\delta^{13}C$ values measured for toluene and benzene sampled in groundwater through piezometers labeled P or Pz (see in Figs. 2–4).This direction of the pollution plume defines the pollution plume coordinate relative to the reactive barrier. The pollution plume coordinate (X axis) represents the algebraic distance between the reactive barrier and the position of the collar where $\delta^{13}C$ values are collected, within the direction of the aquifer flow.The 0 coordinates (Y-X axis intercept) is where the front line of the PRB is installed. Negative coordinates in the X axis (m) are located upstream the flow of the pollution plume (toward the former tank installation) whereas positive coordinates (m) in the X axis are located downstream the flow of the pollution plume relative to the PRB.Linear regressions for $\delta^{13}C$ values are provided to calculate the average percentage of mass loss ML [%] (Eqs. 12b and 12c) and the 1st order rate biodegradation constant, k (Eqs. 13e and 13f) along the pollution plume, based on the $\delta^{13}C_{CO2}$ product and $\delta^{13}C_{TOLUENE}$ substrate monitoring, both.

$\delta^{13}C_{HYDROCARBON}$) = −2.0 ‰ and − 0.9 ‰, for toluene and benzene, respectively, at PRB 0 coordinate (Fig. 5). This difference observed is also due to preferential selection of light isotopes (^{12}C) during bacterial metabolism leading to ^{13}C depletion of CO_2 produced and then released at ground surface.

Geophysical methods (electrical resistivity and induced polarization: Noel et al., 2016b) combined with gas analyses (CO_2 fluxes mainly: Guimbaud et al., 2016) have demonstrated that the amplitude of natural biodegradation changes due to seasonal variations is much more pronounced at the all scale of the pollution plume than at the scale of the PRB (local effect around or downstream of the PRB) during the period of investigation.

According to this point mentioned above, the percentage mass loss of the hydrocarbon substrate (ML, in %, given in Eqs. 12 along the axis of the pollution plume) is best determined at the relevant scale of the site with the aim to identify a seasonal variation. Linear enrichment of $\delta^{13}C_{BT}$ (and thus $\delta^{13}C_{CO2}$) heavy isotopes as a function of the distance to the source is expected for biodegradation in a contaminant plume (Aelion et al., 2010). Due to the few numbers of collars set right above the axis of the pollution plume and the precision given for $\delta^{13}C_{CO2}$ and $\delta^{13}C_{BT}$ data along the axis of the pollution plume, attenuation rate for hydrocarbon degradation is not given between two monitoring collars (or wells as commonly done) but along the axis the pollution plume by reporting each collar position as a function of a pollution plume coordinate. Then, a linear function is adjusted along the axis of the pollution plume. From data shown in Figs. 5 and 6a–c, best fit is confirmed to be linear for the $\delta^{13}C_{CO2}$ and $\delta^{13}C_{BT}$ trend as a function of the pollution plume coordinate. However, linear regression of $\delta^{13}C_{CO2}$ values as a function of plume coordinates is significant at the 0.05 level (p-value) only in 05/06/2014 (0.01), 10/07/2014 (0.03) and 12/02/2014 (0.04) and at the 0.1 level (p-value) in 07/01/2014 (0.10) and 02/03/2015 (0.08), when higher emission of CO_2 lead to higher precision on $\delta^{13}C_{CO2}$ values (summer or early falls) or when experimental conditions (stable weather conditions) lead to more frequent and accurate data (See Figs. 5 and 6a–c for R^2 and p values). Linear regression becomes significant at the 0.05 level for Fig. 6a and b using their whole dataset due to the higher number of data points used, but with degraded R^2 values (R^2 = 0.20, p-value = 0.015 for Fig. 6a: R^2 = 0.14, p-value = 0.019 for Fig. 6b) because this aggregation approach is not theoretically justified due to the overall degradation rate of hydrocarbons which depends on a seasonal cycle. This linear trend is disrupted just above the PRB where fresh deeper hydrocarbons (with lower $\delta^{13}C_{hydrocabon}$ value) may have migrated to the upper bioactive layer from pumping wells. Low spatial resolution for $\delta^{13}C_{CO2}$ above and just around the PRB is explained by the too few effective hours per day available for measurements on that site and priority has been focused to perform measurements at the scale of the pollution plume area. Therefore, quantification of the bioremediation efficiency at the resolution scale of the PRB had to be suppressed as mentioned above, but could be discussed from additional observations.

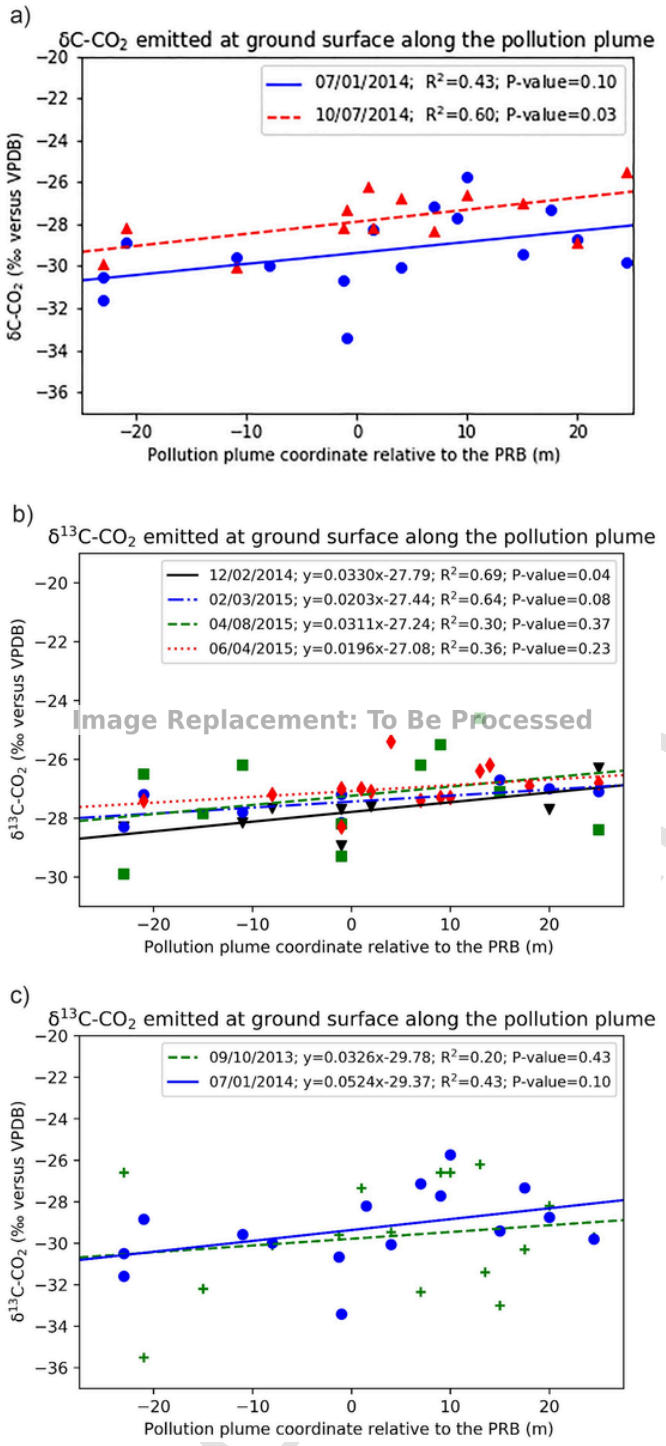

Fig. 6. $\delta^{13}C_{CO2}$ values (‰ versus VPDB) as a function of pollution plume coordinate (m),
These data sets are showing the $\delta^{13}C_{CO2}$ trends, with fitted linear functions used to calculate the average 1st order biodegradation rate constant k for each campaign date. The Y axis represents $\delta^{13}C_{CO2}$ values measured from chamber experiments (‰ versus VPDB) at ground surface along the pollution plume. Similar labeled (squares, circles, diamonds, crosses) are data collected during the same campaign (labeled at the first day of the 2 days campaign).a) July 1 and October 7, 2014 data set, after activation of the PRB.December 2014, February, April and June 2015 data set, showing CO_2 $\delta^{13}C$ trends after activation of the PRB.September 2013 and July 2014 data set, comparing $\delta^{13}C_{CO2}$ trends over a larger previous period, before and after activation of the PRB.

3.2. Biodegradation rate of the groundwater residual hydrocarbon substrate

The percentage of mass loss for the pool of hydrocarbon substrates ML [%] and the 1st order biodegradation rate constant, k, are determined (i) from Eqs. 12b and 13e respectively, based on the $\delta^{13}C_{CO2}$ product monitoring and (ii) from Eqs. 12c and 13f respectively, based on the $\delta^{13}C_{TOLUENE}$ substrate monitoring. ML and k values are determined by using the kinetic fractionation factor of CO_2 relative to the most reactive substrates (TEX) estimated in the water aquifer ($\alpha = 0.9979$ or $\varepsilon = -2.1$‰) from the CSIA data base (U.S. EPA., 2008) (approach ii used for data presented in Table 2 and 5). Approach ii is consistent with the other possible approach (i) made in earlier section: measurements in the field of an overall $\alpha_{app} = 0.997$ (obtained from $\Delta(\delta^{13}C_{CO2} - \delta^{13}C_{BTEX}) = -3$ ‰) and of a fractionation factor due to selective vertical diffusion of the lighter isotope of CO_2 product from the top layer of groundwater to the ground surface (α_{diff}, of 0.9993 or $\varepsilon_{diff} = -0.7$‰), resulting then to the kinetic fractionation factor of CO_2 relative to TEX estimated in the water aquifer from Eq.8: ($\alpha = 0.9993$ or $\varepsilon = -2.3$‰), similar to the one estimated from CSIA ($\alpha = 0.9979$ or $\varepsilon = -(2.1 \pm 0.5)$ ‰).

According to previous discussions, ML [% month^{-1}] and k (Years^{-1}) values given in Table 2 are best derived from the linear regression of $\delta^{13}C$ as a function of the pollution plume coordinate in Figs. 5 and 6a–c, where the slope of the fitted linear function provides the $\delta^{13}C$ values of CO_2 or toluene per unit of travelling distance L. The travelling time t of hydrocarbon substrates in ground water between spots are given by the ratio of the travelling distance L and the horizontal velocity, v, of the substrate migration.

ML and k values are discussed for data with p value < 0.1 and to have enough data for significant precision on data sensitivity versus seasonal variation. ML and k maximum values are obtained 6 weeks after the activation of the PRB in May 2014: 7.4(+2.2–1.4) % month^{-1} and 0.92(+0.29–0.17) year^{-1}, and during July and October with closed averaged value: 3.8(+1.1–0.7) % month^{-1} and 0.46(+0.14–0.09) year^{-1}. ML and k minimum values are obtained 10 months after activation of the PRB in mid-winter in February 2015: 1.4(+0.4–0.3) % month^{-1} and 0.17(+0.05–0.03) year^{-1}. These values are close or lower than the one obtained 6 months before activation the PRB in September 2013: 2.2(+0.7–0.4) % month^{-1} and 0.27(+0.09–0.05) year^{-1}.

In addition, k values obtained after the activation of the PRB in May and December 2014 from $\delta^{13}C_{CO2}$ monitoring: 0.92(+0.29–0.17) year^{-1} and 0.28(+0.08–0.06) year^{-1}, respectively, are consistent with the ones obtained from simultaneous $\delta^{13}C_{TOLUENE}$ monitoring: 0.78 (+0.24–0.15) year^{-1} and 0.44(+0.13–0.09) year^{-1}, according to the precision on $d(\delta^{13}C)/d(L)$ (‰ m^{-1}) derived from the linear regression on each data set. Indeed, ML and k precision depends also on the precision on $d(\delta^{13}C)/d(L)$ (‰ m^{-1}) derived from the linear regression of the linear fit (±5 to 30%) linked to precision on each $\delta^{13}C_{CO2}$ value (±0.15‰ at the best), all best obtained in summer for the highest flux of CO_2. Precision decays in winter and in early spring due to lower precision for individual $\delta^{13}C_{CO2}$ determination from *Keeling* plot approach. The small fluxes of CO_2 in that periods increases the duration (from 5 to 30 min) for enough CO_2 accumulation (usually up to 800 ppmv) in the chamber for accurate $\delta^{13}C_{CO2}$ value determination from *Keeling* plot approach, competing then with the stability drift of the instrument. In addition, in such small flux conditions, linear fits used less numbers of $\delta^{13}C_{CO2}$ values at low active seasons because of this longer period needed to obtain one $\delta^{13}C_{CO2}$ value, acknowledging that each field campaign were limited to the same duration (7 to 8 effective hours per day).

The similar simultaneous $\delta^{13}C$-trends for Toluene and Benzene and $\delta^{13}C$-trends for CO_2 along the GW path coordinates as well as the agreement of first order attenuation rate constants derived from $\delta^{13}C$-trend for CO_2 with the one derived from $\delta^{13}C$-trend for Toluene (considered as a representative hydrocarbon for attenuation rate of gasoline compounds in the contaminated site) argue that ^{13}C enrichment of CO_2

Table 2
Average % mass loss per month, ML [% month^{-1}], and first order biodegradation rate constant, k (year^{-1}), along the pollution plume, assuming fractionation factors $\varepsilon = (-2.1 \pm 0.5)$ ‰ from TEX as representative petroleum hydrocarbons monitored by $\delta^{13}C_{CO2}$ released at ground surface; ML and k values are compared with the one monitored by $\delta^{13}C_{TOLUENE}$ sampled in groundwater, as assumed to be the most representative substrate being degrading in ground water.

	Linear regression information					ML [% month^{-1}] for ε =			k (Years^{-1}) for ε =		
Date Month/Day/Year	Species	d(δ^{13}C)/d(L) ‰ m^{-1}	δ^{13}C at PRB ‰	R^2	*p*-value	−2.6 ‰	−2.1 ‰	−1.6 ‰	−2.6 ‰	−2.1 ‰	−1.6 ‰
09/10/2013	CO_2	0.0326	−29.78	0.04	0.43	1.8	2.2	2.9	0.22	0.27	0.36
05/06/2014	CO_2	0.1107	−28.76	0.78	0.01	6.0	7.4	9.6	0.75	0.92	1.21
05/06/2014	TOLUENE	0.0931	−26.74	0.41	0.06	5.1	6.3	8.1	0.63	0.78	1.02
07/01/2014	CO_2	0.0524	−29.37	0.19	0.10	2.9	3.6	4.7	0.35	0.44	0.57
10/07/2014	CO_2	0.0574	−27.88	0.36	0.03	3.2	3.9	5.1	0.39	0.48	0.63
12/02/2014	CO_2	0.0332	−27.79	0.48	0.04	1.8	2.3	3.0	0.22	0.28	0.36
12/02/2014	TOLUENE	0.0525	−27.03	0.62	0.02	2.9	3.6	4.7	0.35	0.44	0.57
02/03/2015	CO_2	0.0203	−27.44	0.41	0.08	1.1	1.4	1.8	0.14	0.17	0.22
04/08/2015	CO_2	0.0311	−27.24	0.09	0.37	1.7	2.1	2.8	0.21	0.26	0.34
06/04/2015	CO_2	0.0196	−27.08	0.13	0.23	1.1	1.4	1.8	0.13	0.16	0.21

along the pollution plume is more triggered from BTEX biodegradation (toluene mainly) than ^{13}C enrichment of CO_2 produced from possible indirect processes implying methanogenesis intermediates.

3.3. Seasonal variation of the biodegradation rate and effect of the PRB

3.3.1. Seasonal variation of the biodegradation rate

Fig. 7 presents the CO_2 average flux (µmol m^{-2} s^{-1}) along the pollution plume (upstream, above and downstream the PRB). CO_2 emission intensity is also a proxy of biodegradation efficiency. For a better visualization, the Y-X axis intercept is set on March 27, 2014 which is the starting date for the activation of the PRB.

CO_2 emissions are observed to be stimulated during the high microbial activity season (September 2013, June, July and August 2014, June 2015), varying in a similar way downstream, above and upstream the PRB, from 5 to 45 µmol m^{-2}·s^{-1}, from winter to summer. CO_2 emissions are correlated to the annual cycle of the soil temperature and anti-correlated with the groundwater table level (Guimbaud et al., 2016; Noel et al., 2016a), in agreement with stimulation factors of biodegradation efficiency (temperature increase).

First order attenuation rate constant k (Table 2) are mainly correlated with the seasonal variation of CO_2 fluxes (Fig. 7), where max values are in summers and min values in winters, except for June 2015 where k value derived from $d(\delta^{13}C)/d(L)$ has high level of imprecision (*p*-value = 0.23). Both values seasonal variation is mainly due to the annual cycle of the natural biodegradation activity at the scale of the pollution plume.

3.3.2. Effect of the PRB on the biodegradation rate

k and CO_2 fluxes values rise after activation of the PRB due to possible biodegradation stimulation. Indeed, geophysics measurements in Noel et al. (2016b) argued that an efficient natural biodegradation already prevails before activation of the PRB.

Despite $\delta^{13}C_{CO2}$ low spatial resolution that do not cover the zone affected by the biostimulation and the short duration of the biostimulation (~ 1 year), a CO_2 flux increase (Fig. 7) and a $\delta^{13}C_{CO2}$ decrease or some more negative value (Fig. 6a–c) are observed above the PRB, meaning that possible effect of the PRB can be discussed hereafter:

-1) After aerobic biostimulation, CO_2 emissions increase significantly just above the PRB relative to upstream and downstream the bar-

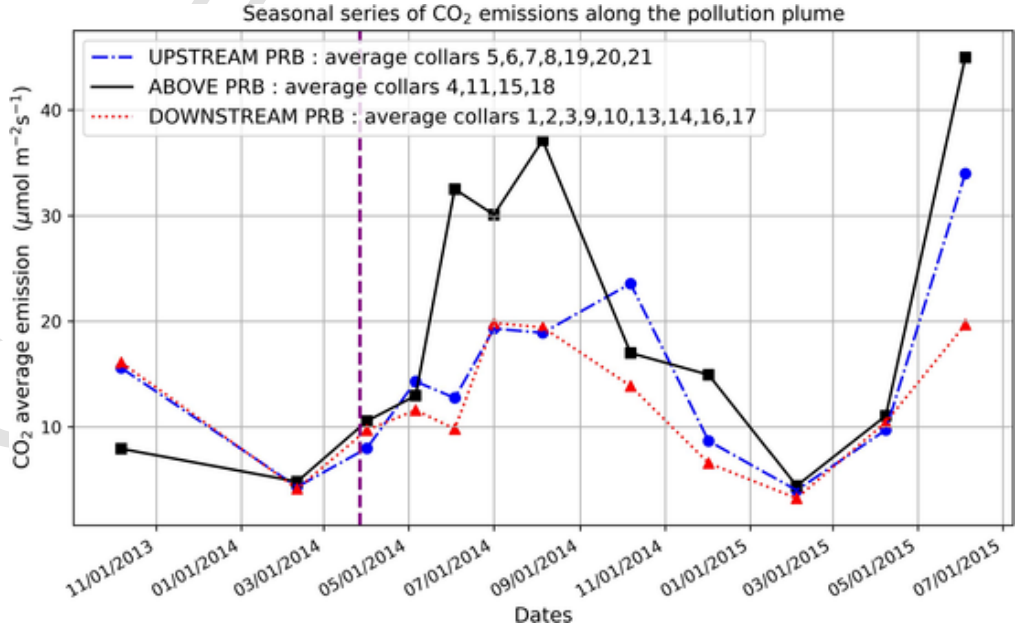

Fig. 7. CO_2 average flux (µmol m^{-2} s^{-1}) along the pollution plume (upstream, above and downstream the Permeable bioRremediation Barrier) versus time, showing that after aerobic bioactivation a more active biodegradation above the PRB occurs in summers. Aerobic Biostimulation started on March 27, 2014 (Y-X axis intercept).

rier during the highest season (summer 2014, and June 2015 in Fig. 7). This is also shown from data provided in Table 3. Table 3 presents the average changes of CO_2 fluxes over a one-year lapse time, i.e. the ratio "year +1 average flux" to "year flux" at given date for upstream, above and downstream the PRB. The one-year lapse time is chosen for ratios to remove seasonal variation of natural biodegradation in order to provide a better evaluation of the stimulated bioremediation efficiency (started on March 27, 2014). Ratio of average flux are the highest above the PRB when calculated after biostimulation relative to before biostimulation (3.9, 2.6 and 3.5 in Sep. 14, Oct. 14 and Feb. 15, respectively). Late effect of the PRB is also observed downstream the pollution plume. More than one year after aerobic biostimulation the ratio of average flux in 2015 (2.1, 1.2, 2.4) reached higher values than in 2014 (1.0 and 1.2).

-2) More negative values of $\delta^{13}C_{CO2}$ observed at ground surface above the reactive barrier after biostimulation (Fig. 6a–c) may be explained by possible remobilization of fresh unreacted contaminants (BTEX) from the lower to upper level of the saturated zone of the aquifer. Table 4 presents the BTEX concentration (mg L^{-1}) measured as the main hydrocarbon substrates in the groundwater. Surface aquifer BTEX concentration reported along the axis of the pollution plume increased above and near the PRB after its treatment starting in March 27, 2014, within the accuracies given for data in Table 4. The consequence could be an underestimation (more negative values observed than expected) for the $\delta^{13}C_{CO2}$ emissions after biostimulation above and downstream the PRB leading to degraded R^2 values for linearity observed in Fig. 6a–c.

One can note that CO_2 fluxes combined with isotopic analysis are complementary to interpret biodegradation processes at the scale of the PRB. Indeed, in the basis of isotopic analysis only, no effect of the PRB on the biodegradation efficiency would have been specifically noticed as a result of the two following observations: (i) Summer k value obtained in September 2013 (p-value = 0.43) is note accurate enough to compare with summer 2014 k values (Fig. 6c) and (ii) the only ground water BTEX analysis performed before and at early stage of the BIOPHY project was a Benzene $\delta^{13}C$ analysis performed on June 1, 2012, exhibiting similar $d(\delta^{13}C)/d(L)$ value (0.0345; R^2 = 0.77) than in April 2014 (0.0240; R^2 = 0.78) and May 2014 (0.0404; R^2 = 0.59) and December 2014 (0.0331; R^2 = 0.13), arguing that the activation of the PRB did not have an obvious effect on benzene biodegradation.

Table 3
Average changes of CO_2 fluxes over one-year lapse time: average and mean deviation of the ratio "year +1 flux" to "year flux" at given date for upstream, above and downstream the bioremediation barrier.

	Sep. 14 / Sep. 13	Oct. 14 / Oct. 13	Feb. 15 / Feb. 14	Apr. 15 / Apr. 14	Jun. 15 / Jun. 14
Upstream	1.6 ± 0.2	1.9 ± 0.6	1.7 ± 0.5	1.6 ± 0.2	N/A
PRB	3.9 ± 1.1	2.6 ± 0.7	3.5 ± 0.8	1.4 ± 0.3	2.0 ± 0.6
Downstream	1.0 ± 0.1	1.2 ± 0.2	2.1 ± 0.4	1.2 ± 0.2	2.4 ± 0.3
Status	After relative to before bioactivation			After biostimulation	

Table 4
BTEX concentration (mg L^{-1}) measured in the groundwater along the axis coordinate of the pollution plume; Accuracies are given at 30% level (Blessing and Saada, 2013; Verardo, 2016). Negative coordinates are located upstream the flow of the pollution plume relative to the bioactive barrier.

Piezo N°	Pz2	Pz24	Pz29	P1
Axis coordinate (m)	−20.5	−7	−1.5	9
Apr. 2015	17.4	27.0	34.2	25.8
Feb. 2015	22.6	18.7	35.2	20.1
Dec. 2014	24.2	13.4	30.0	32.1
Oct. 2014	12.2	7.6	34.1	23.5
Jul. 2014	6.2	6.9	68.3	19.9
Feb. 2014	9.1	3.7	11.4	10.3

4. Conclusions and perspectives

It has been demonstrated that natural remediation efficiency of contaminated soil aquifers by gasoline hydrocarbons (BTEX mainly) can be quantified using the *Rayleigh* equations for $\delta^{13}C_{CO2}$ released at ground surface above the pollution plume, instead of usual approaches based on groundwater hydrocarbons $\delta^{13}C$ analysis, when physical and chemical properties for the contaminated site are appropriate. The validation approach for that specific site is discussed and verified by comparison of first order attenuation rate constant determined from $\delta^{13}C_{CO2}$ analysis emitted at ground surface and from $\delta^{13}C_{TOLUENE}$ analysis in ground water and also supported by seasonal variation of CO_2 flux analysis in that field.

First order biodegradation rate constants (and annual variation) calculated from this approach shows max values after the activation of the PRB in May 2014: 0.92(+0.29–0.17) $year^{-1}$, and during July and October: 0.46(+0.14–0.09) $year^{-1}$ and minimum values in mid-winter in February 2015: 0.17(+0.05–0.03) $year^{-1}$. These values are close or lower than the one obtained before activation the PRB in September 2013: 0.27(+0.09–0.05) $year^{-1}$, supporting that biodegradation still remained process under anaerobic reducing conditions, as it was before activation of the PRB during natural attenuation. First order biodegradation rate constants values are triggered by seasonal variation of microbial activities rather than activation of the PRB at the scale of the pollution plume.

These first order biodegradation rate constants (0.14–1.21 $year^{-1}$) are in the lower range with reported in literature for similar contaminated sites (1.6–18 $year^{-1}$) considering natural attenuation under sulfate reducing conditions.

As regards improvements for fields' studies and investigation (for that and future sites):

(i) higher spatial resolutions analysis with an extension period would have been needed to assess the bioremediation efficiency around the PRB. Due to the large spatial variability of CO_2 flux and $\delta^{13}C$ measured (also linked to a large spatial inhomogeneity of biodegradation, soil structure and diffusivity), higher spatial resolution for samples (grid of 5 m or less instead of 10 m around the bioremediation barrier) would have been needed for that specific site to get a better precision on biodegradation rate constant values and to assess the bioremediation efficiency around the PRB. Remediation process should have been pursued for a longer period (at least until end of 2015) to assess the relative efficiency of this bioactivation through a significant migration plume distance and the post effect after steady state remobilization of BTEX in the upper layer of the aquifer. Indeed, the important delay for the settlement of the pilot site within the limited period of the ANR-ECOTECH-BIOPHY project and the short periods available for investigation (1 day.$month^{-1}$ in average) had limited spatial resolution and the period of measurements after bioactivation. One can note that such spatial resolution and delay are less needed for homogenous soils structure or for natural attenuation, by opposition to Enhanced Bioremediation where the installation of the treatment process (PRB or other techniques) may remobilize contaminants leading to complex interpretation of the dynamic process of biodegradation. This remobilization problematic is unfortunately common to whatever kind of the approach (substrate or product) used for biodegradation monitoring.

(ii) To improve assessment of bioremediation rate kinetic, more accurate values of ε fractionation factor for the representative hydrocarbon contaminants are also required. As a consequence, more experiments need to be done in surrogate soils and pollutants on large laboratory well characterized soil macrocosms. Such soil experimental platform is under construction at BRGM within the joint Region Centre – Europe funded project "ARD2020 PIVOTS-PRIME".

As regards economical aspect, the ability to quantify the biodegradation rate of hydrocarbons in a contaminated aquifer using the $\delta^{13}C_{CO2}$ approach analysis is of great interest. The $\delta^{13}C_{CO2}$ online surface gas mon-

itoring approach is an efficient substitute of the classical methods where the monitoring of groundwater hydrocarbon substrates $\delta^{13}C$ analysis requires land manipulations and underground sampling. $\delta^{13}C_{CO2}$ surface gas monitoring is fast to be set up and of low-cost installation because no boreholes or wells have to be dug and only movable manual chambers are needed. Therefore, $\delta^{13}C_{CO2}$ surface gas monitoring provides fast analysis of the status of the contaminated sites, if mechanisms of CO_2 production and transfer could be understood. A strong economic interest can be found in this gas monitoring approach: the best cost efficiency policy for the choice of the remediation process for contaminated hydrocarbon sites in agreement with the future use of lands; fast adaptation of biotreatment can be also done in real time if needed.

Uncited references

Alvarez De Pedro and Ilman, 2005

Declaration of Competing Interest

The authors declare that they have no known competing financial interests or personal relationships that could have appeared to influence the work reported in this paper.

Data availability

Data will be made available on request.

Acknowledgments

This research is conducted at OSUC (Observatoire des Sciences de l'Univers en Région Centre – Centre National de la Recherche Scientifique – Université d'Orléans) and supported by the funded project of the French Research Agency: ECOTECH BIOPHY (Optimisation de procédés de BIOdépollution des eaux souterraines contaminées par des hydrocarbures par un monitoring géoPHYsique et analyse de gaz en ligne) (ANR-10-ECOT-014). BIOPHY project aimed at demonstrating the feasibility to monitor petroleum-hydrocarbon biodegradation in a contaminated aquifer from a gasoline station near Paris in France by combining two non-intrusive methods (i) – geophysics (soil electric resistivity, capacity) and (ii) – ground surface analysis of the CO_2 biodegradation product (fluxes with $\delta^{13}C$ determination) released from remaining hydrocarbon substrates (BTEX Mainly).

This work is also supported by the LABEX VOLTAIRE (LABoratoire d'EXcellence VOLatils – Terre, Atmosphère et Interactions – Ressources et Environnement) (ANR-10-LABX-100-01) and the AMIS (FAte and IMpact of AtmospherIc PollutantS) project funded by the European Union, under the Marie Curie Actions IRSES (International Research Staff Exchange Scheme), within the Seventh Framework Programme FP7-PEOPLE-2011-IRSES and by The MARSU "MARine atmospheric Science Unravelled: Analytical and mass spectrometric techniques development and application" project funded by the European Union's Horizon 2020 Research and Innovation program – Marie Skłodowska-Curie Actions (H2020-MSCA-RISE-2015-690958).

The SPIRIT-BIOPHY instrument is integrated within the French Research Organisations ARD2020 PIVOTS (2016-21): « Plateformes d'Innovation, de Valorisation et d'Optimisation Technologique environnementaleS » funded by Region Centre, CPER, FEDER, French Research Organisations, within the Platform « PRIME »: pour la « Remédiation et l'Innovation au service de la Métrologie Environnementale » (remediation processes of contaminated soils and aquifers).

We gratefully acknowledge the engineering and technical staffs of the LPC2E, G. Chalumeau, M. Chartier, S. Chevrier, P. Jacquet, C .Robert, F. Savoie, T. Vincent, for their contribution to SPIRIT-BIOPHY development and maintenance or their participation in various field campaigns. We also thank SERPOL and TOTAL which managed the field study site for bioremediation.

References

Abreu, L.D.V., Johnson, P.C., 2006. Simulating the effect of aerobic biodegradation on soil vapor intrusion into buildings: influence of degradation rate, source concentration, and depth. Environ. Sci. Technol. 40, 2304–2315.

Aelion, C., Hoehener, P., Hunkeler, D., Aravena, R., 2010. Environmental Isotopes in Biodegradation and Bioremediation. CRC Press, USA.

Ahad, J. M. E., Sherwood Lollar, B., Edwards, E. A., Slater, G. F., Sleep, B. E., 2000. Carbon isotope fractionation during anaerobic biodegradation of toluene: Implications for intrinsic bioreme diation. Environmental Science Technology 34, 892.

Alvarez De Pedro, J., Ilman, W.A., 2005. Bioremediation and Natural Attenuation: Process Fundamentals and Mathematical Models. Wiley editions, ISBN 978-0-471-65043-0.

Atteia, O., Guillot, C., 2007. Factors controlling BTEX and chlorinated solvents plume length under natural attenuation conditions. J. Contam. Hydrol. 90, 81–104.

Barona, A., Elias, A., Arias, R., Acha, E., Cano, I., 2007. Desorption and biofiltration for the treatment of residual organic gases evolved in soil decontamination processes. Chem. Eng. Technol. 30, 1499–1505.

Bauer, S., Beyer, C., Kolditz, O., 2006. Assessing measurement uncertainty of first-order degradation rates in heterogeneous aquifers. Water Resour. Res. 42. . W01420.

Bekins, B.A., Warren, E., Godsy, E.M., 1998. A comparison of zero-order, first-order, and monod biotransformation models. Ground Water 36, 261–268.

BenIsrael, M., Wanner, P., Aravena, R., Parker, B.L., Haack, E.A., Tsao, D.T., Dunfield, K.E., 2019. Toluene biodegradation in the vadose zone of a poplar phytoremediation system identified using metagenomics and toluene-specific stable carbon isotope analysis. Int. J. Phytoremediation 1–10.

Blessing, M., Saada, A., 2013. Projet ATTENA - Guide Méthodologique pour l'utilisation des approches isotopiques dans le cadre de la démonstration d'atténuation naturelle. (ADEME - BRGM).

Bouchard, D., Hohener, P., Hunkeler, D., 2008a. Carbon isotope fractionation during volatilization of petroleum hydrocarbons and diffusion across a porous medium: a column experiment. Environ. Sci. Technol. 42, 7801–7806.

Bouchard, D., Hunkeler, D., Gaganis, P., Aravena, R., Hohener, P., Broholm, M.M., Kjeldsen, P., 2008b. Carbon isotope fractionation during diffusion and biodegradation of petroleum hydrocarbons in the unsaturated zone: field experiment at Vaerlose airbase, Denmark, and modeling. Environ. Sci. Technol. 42, 596–601.

Catoire, V., Robert, C., Chartier, M., Jacquet, P., Guimbaud, C., Krysztofiak, G., 2017. The SPIRIT airborne instrument: a three-channel infrared absorption spectrometer with quantum cascade lasers for in-situ atmospheric trace-gas measurements. Appl. Phys. B Lasers Opt. 123 (9), 12.

Cerling, T.E., Solomon, D.K., Quade, J., Bowman, J.R., 1991. On the isotopic composition of carbon in soil carbon dioxide. Geochim. Cosmochim. Acta 55, 3403–3405.

Conrad, M.E., Daley, P.F., Fischer, M.L., Buchanan, B.B., Leighton, T., Kashgarian, M., 1997. Combined C-14 and delta C-13 monitoring of in situ biodegradation of petroleum hydrocarbons. Environ. Sci. Technol. 31, 1463–1469.

Cozzarelli, I.M., Bekins, B.A., Eganhouse, R.P., Warren, E., Essaid, H.I., 2010. In situ measurements of volatile aromatic hydrocarbon biodegradation rates in groundwater. J. Contam. Hydrol. 111, 48–64.

Craig, H., 1954. Carbon 13 in plants and the relationships between carbon 13 and carbon 14 variations in nature. J. Geol. 62, 115–149.

Davis, G.B., Barber, C., Power, T.R., Thierrin, J., Patterson, B.M., Rayner, J.L., Wu, Q., 1999. The variability and intrinsic remediation of a BTEX plume in anaerobic sulphate-rich groundwater. J. Contam. Hydrol. 36 (3), 265–290.

De Robert, E.W., 2006. Principles and Practice of Soil Science: The Soil as a Natural Resource, Fourth edition. Blackwell Sciences Ltd, a Blackwell Publishing Company.

Denk, T.R.A., Mohn, J., Decock, C., Lewicka-Szczebak, D., Harris, E., Butterbach-Bahl, K., Kiese, R., Wolf, B., 2017. The nitrogen cycle: a review of isotope effects and isotope modeling approaches. Soil Biol. Biochem. 105, 121–137.

El-Naas, M.H., Acio, J.A., El Telib, A.E., 2014. Aerobic biodegradation of BTEX: progresses and prospects. J. Environ. Chem. Eng. 2, 1104–1122.

Elsner, M., Zwank, L., Hunkeler, D., Schwarzenbach, R., 2005. A new concept linking observable stable isotope fractionation to transformation pathways of organic pollutants. Environ. Sci. Technol. 39, 6896–6916.

Fischer, A., Theuerkorn, K., Stelzer, N., Gehre, M., Thullner, M., Richnow, H.H., 2007. Applicability of stable isotope fractionation analysis for the characterization of benzene biodegradation in a BTEX contaminated aquifer. Environ. Sci. Technol. 41, 3689–3696.

Guimbaud, C., Catoire, V., Gogo, S., Robert, C., Laggoun-Défarge, F., Chartier, M., Grossel, A., Albéric, P., Pomathiod, L., Nicoullaud, B., Richard, G., 2011. A portable infrared laser spectrometer for field measurements of trace gases. Meas Sci Technol 22, 1.

Guimbaud, C., Noel, C., Chartier, M., Catoire, V., Blessing, M., Gourry, J.C., Robert, C., 2016. A quantum cascade laser infrared spectrometer for CO_2 stable isotope analysis: field implementation at a hydrocarbon contaminated site under bioremediation. J. Environ. Sci. 40, 60–74. . special issue "Changing complexity of air pollution." .

Johnson, S.J., Woolhouse, K.J., Prommer, H., Barry, D.A., Christofi, N., 2003. Contribution of anaerobic microbial activity to natural attenuation of benzene in groundwater. Eng. Geol. 70 (3–4), 343–349.

Kolhatkar, R., Schnobrich, M., 2017. Land application of sulfate salts for enhanced natural attenuation of benzene in groundwater: a case study. Groundwater Monit. Remediat. 37 (2), 43–47.

Landmeyer, J.E., Vroblesky, D.A., Chapelle, F.H., 1996. Stable carbon isotope evidence of biodegradation zonation in a shallow jet-fuel contaminated aquifer. Environ. Sci.

Technol. 30, 1120–1128.
Lari, K.S., Davis, G.B., Rayner, J.L., Bastow, T.P., Puzon, G.J., 2019. Natural source zone depletion of LNAPL: a critical review supporting modelling approaches. Water Res. 157, 630–646.
Luo, H., Dahlen, P., Johnson, P.C., Peargin, T., Creamer, T., 2009. Spatial variability of soil-gas concentrations near and beneath a building overlying shallow petroleum hydrocarbon–impacted soils. Ground Water Monit. Remediat. 29, 81–91.
Mancini, S. A., Ulrich, A. C., Lacrampe-Couloume, G., Sleep, B. E., Edwards, E. A., Sherwood Lollar, B., 2003. Carbon and hydrogen isotopic fractionation during anerobic biodegradation of benzene. Applied Environment Microbiology 69, 191.
Mariotti, A., Germon, J.C., Hubert, P., Kaiser, P., Letolle, R., Tardieux, A., Tardieux, P., 1981. Experimental determination of nitrogen kinetic isotope fractionation: some principles; illustration for the denitrification and nitrification process. Plant Soil 62, 413–430.
Meckenstock, R. U., Morasch, B., Warthmann, R., Schink, B., Annweiler, E., Michaelis, W., Richnow, H. H., 1999. $^{13}C/^{12}C$ isotope fractionation of aromatic hydrocarbons during microbial degradation. Environmental Microbiology 1, 409.
Morasch, B., Richnow, H. H., Schink, B., Meckenstock, R.U., 2004. Stable isotope fractionation caused by glycyl radical enzymes during bac terial degradation of aromatic compounds. Applied Environmental Microbiology 70, 2935.
Morasch, B., Richnow, H. H., Schink, B., Vieth, A., Meckenstock, R. U., 2001. Stable carbon and hydrogen isotope fractionation during microbial toluene degradation: mechanistic and environmental aspects. Applied Environmental Microbiology 67, 4842.
Neumann, R.B., Blazewicz, S.J., Conaway, C.H., Turetsky, M.R., Waldrop, M.P., 2016. Modeling CH4 and CO2 cycling using porewater stable isotopes in a thermokarst bog in Interior Alaska: results from three conceptual reaction networks. Biogeochemistry 127, 57–87.
Noel, C., Gourry, J.C., Deparis, J., Ignatiadis, I., Battaglia-Brunet, F., Guimbaud, C., 2016a. Suitable real time monitoring of the aerobic biodegradation of toluene in contaminated sand by spectral induced polarization measurements and CO_2 analyses. Near Surf. Geophys. 14, 263–273.
Noel, C., Gourry, J.C., Deparis, J., Blessing, M., Ignatiadis, I., Guimbaud, C., 2016b. Combining geoelectrical measurements and CO_2 analyses to monitor the enhanced bioremediation of hydrocarbon-contaminated soils: a field implementation. Appl. Environ. Soil Sci. 2016, 15. . special issue "Integrated Approaches to Soil Contamination Monitoring". Article ID 1480976.
Pataki, D.E., Ehleringer, J.R., Flanagan, L.B., Yakir, D., Bowling, D.R., Still, C.J., Buchmann, N., Kaplan, J.O., Berry, J.A., 2003. The application and interpretation of Keeling plots in terrestrial carbon cycle research. Glob. Biogeochem. Cycles 17, 1022.
Rayleigh, J.W.S., 1896. Theoretical considerations respecting the separation of gases by diffusion and similar processes. Philos. Mag. 42, 493–498.
Richnow, H.H., Annweiler, E., Michaelis, W., Meckenstock, R.U., 2003. Microbial in situ degradation of aromatic hydrocarbons in a contaminated aquifer monitored by carbon isotope fractionation. J. Contam. Hydrol. 65, 101–120.
Schmidt, T.C., Zwank, L., Elsner, M., Berg, M., Meckenstock, R.U., Haderlein, S.B., 2004. Compound-specific stable isotope analysis of organic contaminants in natural environments: a critical review of the state of the rat, prospects, and future challenges. Anal. Bioanal. Chem. 378, 283–300.
Sra, K.S., Ponsin, V., Kolhatkar, R., Hunkeler, D., Thomson, N.R., Madsen, E.L., Buscheck, T., 2022. Sulfate land application enhances biodegradation in a petroleum hydrocarbon smear zone. Groundwater Monit. Remediat. https://doi.org/10.1111/gwmr.12547.
Thierrin, J., Davis, G.B., Barber, C., Patterson, B.M., Pribac, F., Power, T.R., Lambert, M., 1993. Natural degradation rates of BTEX compounds and naphthalene in a sulphate reducing groundwater environment. Hydrol. Sci. J. 38 (4), 309–322.
Thullner, M., Centler, F., Richnow, H.H., Fischer, A., 2012. Quantification of organic pollutant degradation in contaminated aquifers using compound specific stable isotope analysis – review of recent developments. Org. Geochem. 42, 1440–1460.
Toth, C.R.A., Luo, F., Bawa, N., Webb, J., Guo, S., Dworatzek, S., Edwards, E.A., 2021. Anaerobic benzene biodegradation linked to the growth of highly specific bacterial clades. Environ. Sci. Technol. 55 (12), 7970–7980.
U.S. EPA., 2008. A Guide for Assessing Biodegradation and Source Identification of Organic Ground Water Contaminants Using Compound Specific Isotope Analysis (CSIA). Office of Research and Development, U.S. EPA, Ada, Oklahoma.
Van Breukelen, B.M., 2007a. Extending the Rayleigh equation to allow competing isotope fractionating pathways to improve quantification of biodegradation. Environ. Sci. Technol. 41, 4004–4010.
Van Breukelen, B.M., 2007b. Quantifying the degradation and dilution contribution to natural attenuation of contaminants by means of an open system Rayleigh equation. Environ. Sci. Technol. 41, 4980–4985.
Verardo, E., 2016. Procédés de traitement biologiques in situ: la modélisation numérique comme outil d'aide à la décision. PhD thesis. Université Michel de Montaigne-Bordeaux III.
Verardo, E., Atteia, O., Rouvreau, L., Siade, A., Prommer, H., 2021. Identifying remedial solutions through optimal bioremediation design under real-world field conditions. J. Contam. Hydrol. 237, 103751.
Wanner, P., Aravena, R., Fernandes, J., BenIsrael, M., Haack, E.A., Tsao, D.T., Dunfield, K.E., Parker, B.L., 2019. Assessing toluene biodegradation under temporally varying redox conditions in a fractured bedrock aquifer using stable isotope methods. Water Res. 165, 11.
Wiedemeier, T.H., Rifai, H.S., Newell, C.J., Wilson, J.T., 2007. Natural Attenuation of Fuels and Chlorinated Solvents in the Subsurface. John Wiley & Sons, Inc. editions, ISBN 978-0-471-19749-2, p. 617.
Wilkes, H., Boreham, C., Harns, G., Zengler, K., Rabus, R., 2000. Anaerobic degradation and carbon isotopic fractionation of alkylbeneznes in crude oil by sulphate-reducing bacteria. Organic Geochemistry 31, 101.